Amount and Scattering of Dyes and their Influence on the Photocurrent Enhancement of TiO2 Hierarchically Structured Photoanodes for Dye-Sensitized Solar Cells

Wen-Yao Huang[1], Tung-Li Hsieh[2*]

[1]Department of Photonics, National Sun Yat-sen University, Kaohsiung City, Taiwan (R.O.C.)
[2]General Education Center of Wenzao Ursuline University of Languages
[*]Correspondence to: Tung-Li Hsieh (e-mail: tunglihsieh@gmail.com)
Phone: +886-7-342-6031 and Fax: +886-7-342-7942

Abstract

In this study, we prepared and analyzed the properties of hills-like hierarchically structured TiO_2 photoanodes for dye-sensitized solar cells (DSSCs). We expected that the presence of appropriately aggregated TiO_2 clusters in the photoanode layer would translate in a relatively strong light scattering and dye loading, increasing the photovoltaic efficiency. A detailed light-harvesting study was performed by employing polyvinyl alcohol (PVA) polymers of different molecular weights as binders for the aggregation of the TiO_2 nanoparticles (P-25 Degussa). Hence, we obtained a series of TiO_2 films presenting a variety of morphologies. Their reflection, as well as the absorbance of the attached dye, the amount of dye loading, and the performance of the fabricated DSSC devices were investigated. Our optimized device presenting a relatively high dye loading and well light harvesting ability, and able to enhance the short-circuit current (J_{sc}) in the DSSCs by 23%.

Key words: Hierarchical structure; TiO_2 photoanode; Dye-sensitized solar cell; Light scattering

Introduction

Recently, dye-sensitized solar cells (DSSCs) have attracted much attention [1-9] due to their low production cost and high conversion efficiency. In general, the photoanode of a DSSC is represented by a porous layer: 20-nm TiO_2 particles are coated on a transparent conductive oxide (TCO) glass, and a monolayer of a charge transfer dye is applied to the porous film. Under illumination, the dye molecules become photoexcited and release electrons; these are injected into the conduction band of TiO_2, diffused through the porous layer, and are subsequently collected and transported to the external load by the TCO. Porous TiO_2 electrodes play an important role in improving the performance of DSSCs. In fact, these devices should ideally possess a TiO_2 layer with a high surface area, allowing a large adsorption and well light scattering. These properties translate in an enhanced light harvesting, short-circuit current (J_{sc}), and power conversion efficiency [10]. The research results of Wang et al. [11] demonstrated an obvious decrease of the surface area in association with an increase in particle size. These authors indicated that the use of very small TiO_2 particles was essential to increase the surface area of the TiO_2 layer and increase the amount of dye, while large particles were required to enhance the absorption of red light through light scattering. A simultaneous increase of the surface area and of light scattering is not possible, since these two properties oppose each other. Previous studies have indicated that the aggregation of TiO_2 nanoparticles in a hierarchical structure can improve the performance of DSSCs [12,13]. Moreover, these structured TiO_2 films were found to improve the efficiency of electrolyte diffusion or penetration, presenting high dye loadings, and enhancing the scattering effect. The influence of the amount of dye and its light scattering effect on light harvesting, however, were not discussed in detail.

The Mie theory entails that the intensity of light scattering depends on the size of the illuminated object: the scattering cross section increases with the size of the scattering object. This theory has been conveniently applied to light harvesting in solar cells, especially for longer wavelengths [14-16]. In our study, we aimed to obtain a film characterized by both a high surface area and well light scattering. In order to evaluate the balance between these two factors and their influence on light harvesting, we created a series of hierarchically structured TiO_2 films with different degrees of aggregation (Fig 1). In order to perform a detailed light harvesting study, we employed polyvinyl alcohol (PVA) polymers of different molecular weights as binders for the aggregation of TiO_2 nanoparticles. Hence, we obtained a series of TiO_2 films presenting a variety of morphologies. Their reflection, as well as the absorbance of the attached dye, the amount of dye loading, and the performance of the fabricated DSSC devices were investigated. Finally, we created an optimized device characterized by a relatively high dye loading and well light harvesting ability, and able to enhance the short-circuit current (J_{sc}) in the DSSCs by 23%.

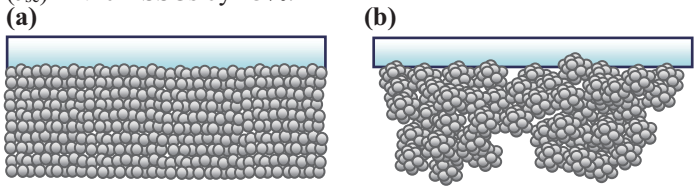

Fig 1 Schematic diagram of (a) conventional film and (b) hierarchical structured film.

Experimental

2.1 Preparation of a hierarchically structured TiO_2 particle paste

A hierarchically structured TiO2 paste was prepared using PVA (CCP) as binders to aggregate TiO2 nanoparticles. The size of the aggregations was regulated by altering the molecular weight (MW = 31,000–99,000) of the polymers. First, 1g of PVA water solution was stirred at 65 °C overnight and dissolved in a mixed solvent (1.0 ml H2O + 0.8 ml ethanol). Then, 0.6 g of TiO2 powder (P-25, 21 nm Degussa) were added to the solution. The resulting suspension was put in an ultrasonic cleaner for 30 min. After 0.05 ml of Triton X-100

ISBN: 978-1-7281-2501-5

and 0.05 ml of acetyl-acetone surfactants were added to the suspension, this was put again in the ultrasonic cleaner for 30 min and then stirred for 24 h.

2.2 Fabrication of the DSSCs

A dense TiO_2 layer about 45 nm was spin-coated on an indium tin oxide (ITO) glass (Merck), which was used as a blocking layer to avoid the recombination due to the I_3^- grabbing photoelectrons on the conducting substrate surface. A TiO_2 porous layer, with an active area of 1.3 × 0.8 cm^2, was formed through this spin-coating process. To induce the evaporation of the solvent, the decomposition of the PVA, and ensure the electrical contact and mechanical adhesion of the TiO_2 films on the glass, these were baked at 100 °C for 10 min, and subsequently calcined at 450 °C for ~ 30 min in the presence of air. The average thickness of the TiO_2 films (~ 10 μm) was checked using an α-step surface profiler. Dye adsorption was achieved by immersing the calcined films in a 5×10^{-4} M ruthenium dye solution, cis-bis(isothiocyanato) bis(2,2'-bipyridyl-4,4'-dicarboxylato) ruthenium(II) bis-tetrabutylammonium (D719 dye, Eversolar), and in a tert-butanol and acetonitrile co-solvent, for 20 h at 25 °C. The dye adsorbed on the TiO_2 films was rinsed with ethanol and dried at 85 °C for 10 min. Pt-coated ITO was used as a counter electrode; subsequently, the dye-adsorbed TiO_2 films were sealed using a hot-melt adhesive (thickness = 30 μm, Surlyn, Tripod). A liquid electrolyte consisting of I_2 (0.1 M), LiI (0.1 M), 1-propyl-2,3-dimethylimidazolium iodide (DMPII, 0.6 M), and 4-tert-butylpyridine (TBP, 0.25 M, Aldrich) in 3-Methoxypropionitrile (MPN, Fluka) was then injected to fill the space between cells.

For the sake of comparison, we also prepared a conventional TiO_2 film (without the addition of PVA) the device as a standard was fabricated equally with above methods.

2.3 Characterization and measurement

The surface morphology of the TiO_2 porous films was observed by field emission gun-scanning electron microscopy (JEOL JSM-6700F). The reflectance and absorbance spectra were measured by an UV-vis spectrometer (Perkin Elmer UV-Vis Lambda35). The photocurrent-voltage of the DSSCs was measured using instead a Keithley 2400 analyser under AM 1.5 simulated illuminations with an intensity of 100 mW/cm^2. A 300 W xenon lamp (MODEL 6258) was used as light source: a filter was applied on it to approximate the sunlight spectrum. The incident photo-to-current conversion efficiency (IPCE) spectra were measured by a self-designed IPCE system, consisting of a xenon lamp (Xe Light source 70051), a monochromator (Cornerstone 13074004), a power measurement (2935-C), a source measurement unit (M3500A), and a power detector (818-SL).

The level of dye adsorption was evaluated by the following method: the dye molecules were desorbed from the TiO_2 layer by rinsing it with a 0.1 M NaOH aqueous solution; then, the absorbance at 511 nm of the dye solution was measured by UV-vis spectrometry, determining its concentration.

Results and Discussion

3.1 Morphologies of the TiO_2 films

In order to determine the optical properties of the TiO_2 films characterized by different degrees of particle aggregation, we used PVA with different molecular weights as binders. These films were expected to present different levels of light reflectance and absorbance, as well as dissimilar morphologies. To verify the presence of aggregations in the paste, we diluted the paste and observed it by SEM (Fig 2). These observations confirmed the presence of numerous micro-aggregations composed of TiO_2 nanoparticles; moreover, the sizes of these aggregations tended to increase with the molecular weights of the PVAs used. We supposed that, in each sample, the interactions between the PVA, the TiO_2 particles, and the surfactant were in a state of static equilibrium. In these stable conditions, numerous uniformly sized TiO_2 aggregations occurred in the paste; additionally, the relationship between their size and the molecular weight of the PVA derived from the interaction between TiO_2 and PVA. In order to investigate the aggregation mechanism, we maintained the same molecular weight, while changing the amount of PVA from 0.2 g to 0.3 g (Fig 3). Despite this change, the size of the aggregations did not vary. Probably, the hydroxyl groups contained in the PVA molecules interacted with those on the TiO_2 particles, forming clusters in the processing paste. These TiO_2-PVA clusters did not aggregate continuously, due to the infuence of the surfactant. When the PVA molecular weight increased, the number of hydroxyl groups in each PVA molecule increased as well: the interaction between the PVA molecules and the TiO_2 particles became stronger, inducing the formation of bigger aggregations in the paste. When a higher amount of PVA molecules was added to the paste, however, the number of hydroxyl groups in each PVA molecule did not change: the addition of PVA did not cause an enlargement of the aggregations, but just increased their number.

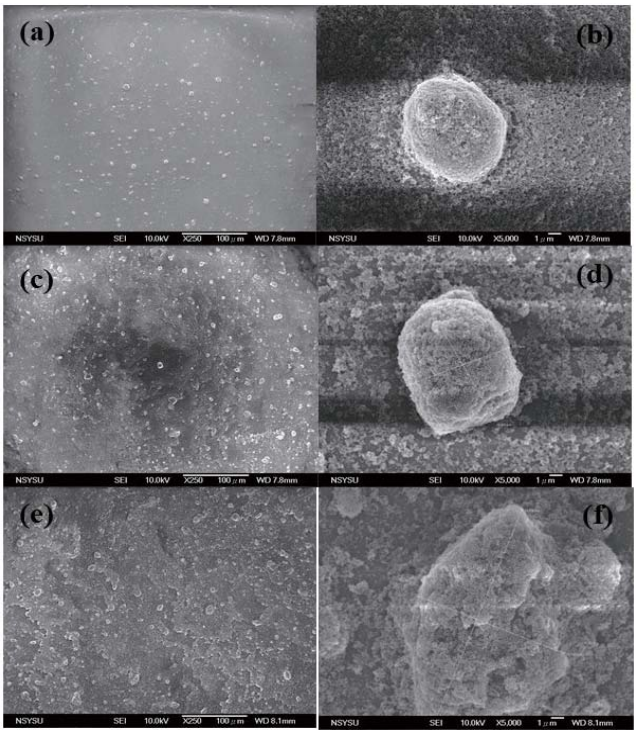

Fig 2 TiO_2 aggregations SEM images from diluted paste. (a), (b) Mw 31,000; (c), (d) Mw 40,000; (e), (f) Mw 54,000.

ISBN: 978-1-7281-2501-5

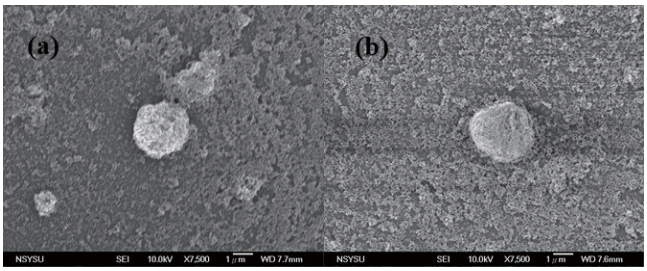

Fig 3 TiO_2 aggregations SEM images from diluted paste with PVA (a) 0.2g, (b) 0.3g

Fig 4 shows the surface (SEM) images of both the conventional and PVA- treated films. The conventional film was created by uniformly stacking the nanoparticles. The size of the TiO_2 aggregations and the porosity of this film were proportional to the molecular weight of the PVA used. From film A to film D, the size of the aggregations increased from ~ 100 nm to 300 nm. These results suggest that the use of PVAs with higher molecular weights induced the formation of larger TiO_2-PVA aggregations in the paste. Relatively big TiO_2 aggregations persisted after coating the substrate and following polymer decomposition (during the calcining process). The side views observed by SEM (Fig 5) revealed that the conventional film possessed a very smooth top surface, while the surfaces of the PVA treated films were hills-like (probably due to the occurrence of TiO_2 micro-clusters). The presence of these micro-nano aggregations in the hierarchically structured TiO_2 film, suggested the idea that such a structure would provide an enhanced light scattering effect.

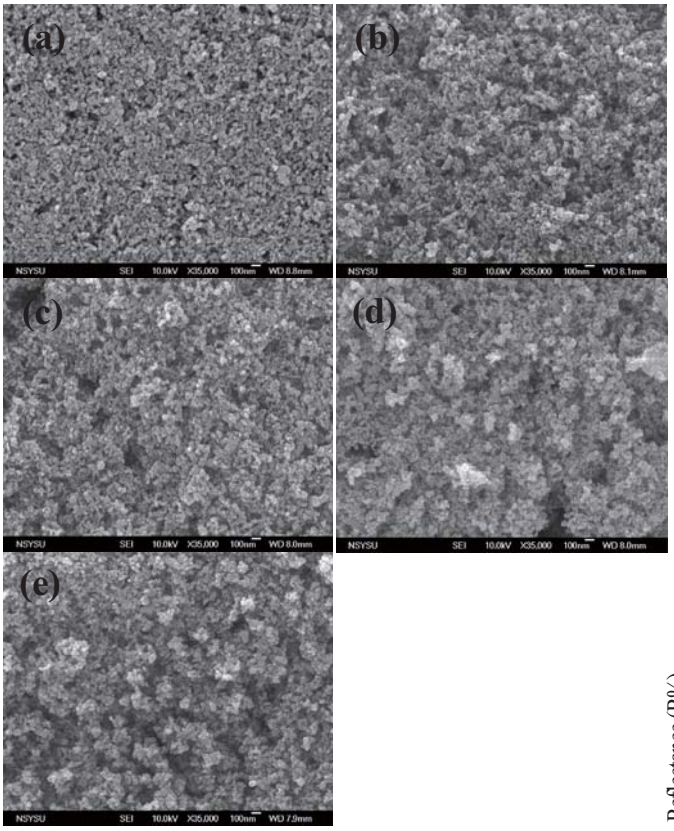

Fig 4 Surface SEM images of (a) conventional TiO_2 film, PVA treated TiO_2 films with (b) Mw 31,000, (c) Mw 40,000, (d) Mw 54,000, and (e) Mw 99,000.

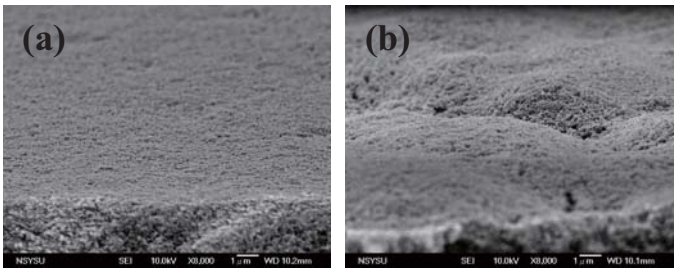

Fig 5 Side views SEM images of (a) conventional film and (b) PVA treated film.

3.2 Optical properties of the TiO_2 films and photoanodes

To determine the light scattering effects of the TiO_2 films, we measured their reflectance (Fig 6a). The reflectance of STD was lower than that of the others, since its uniformly stacked nanoparticles were not able to scatter the incident light efficiently. The PVA-treated films instead, in which the nanoparticles were aggregated forming a hierarchically structured film, provided a higher reflectance. Also the normalized reflectance spectra (Fig 6b) showed some differences. An analysis of the longer wavelength regions in each curve (600 nm – 800 nm) indicated that the size of the aggregations in the samples increased with the reflectance. This phenomenon is in accord with the Mie scattering theory.

So far, several studies have discussed the light reflectance related to the scattering effect of TiO_2 films [15,17]. However, we could not determine how the reflected photons were scattered in the porous films. Our light scattering schematic diagram is shown in Fig7. The incident light was scattered by the nanoparticles and subsequently reflected forward or traversely through the porous film: by measuring only the reflectance, we actually neglect the photons scattered towards and through the film; moreover, it is technically difficult the place a detector in the film for the measurement of the scattering intensity. In this study, the light scattering effect was investigated thoroughly by measuring the unit of dye absorbance. Our objective was in fact to understand how much light was actually absorbed in the film by each dye molecule, as well as to characterize the intensity of the light scattering effect. The absorbance spectra of the dye molecules in the TiO_2 films are shown in Fig 8. These spectra were obtained by deducting the absorbance of the TiO_2 films from the photoanodes (i.e., TiO_2 with dye), and then eliminating the amount of dye on each film. Fig 8 clearly shows that each unit of dye molecule was able to harvest more light in the PVA-treated films, and that the light absorbance of each dye increased with the size of the aggregations. These results indicate that the light scattering effect was significantly stronger in the films containing bigger aggregations.

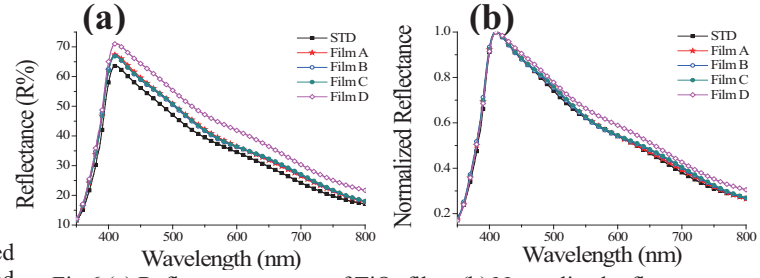

Fig 6 (a) Reflectance spectra of TiO_2 films (b) Normalized reflectance spectra.

ISBN: 978-1-7281-2501-5

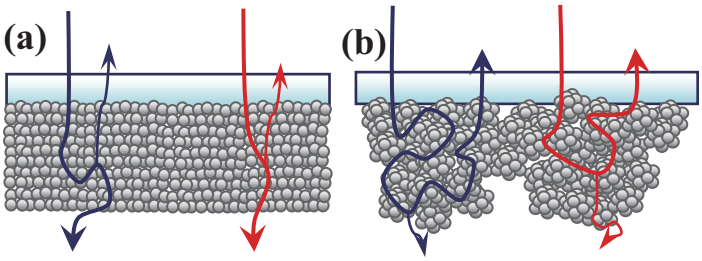

Fig 7 Light scattering schematic diagram of (a) conventional film and (b) hierarchical structured film.

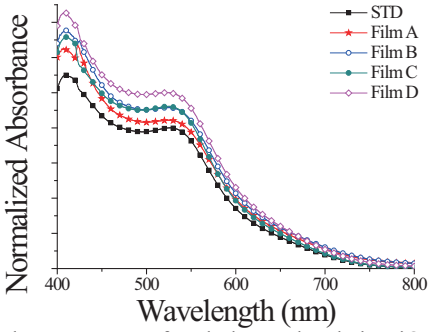

Fig 8 Absorbance spectra of each dye molecule in TiO_2 films

3.3 Performances of the DSSCs

The optical properties of the TiO_2 films having different morphologies have been described in section . Here, we will discuss the performances of the devices in relation to light scattering, which are summarized in Table 1. Devices A to D were fabricated using different TiO_2 films (A to D). We noticed that, when the size of the aggregations increased, the dye amount decreased. This effect was probably linked to the change in surface area: the scattering effect should have increased reflecting the occurrence of larger aggregations. The short-circuit current did not decrease directly from device A to D. In fact, based on the analyses of device C, we identified a turning point in the balance between the amount of dye and the light scattering effect. Moreover, although film D possessed a lower amount of dye 5.81×10^{-8} mol/cm^2 than the conventional film 6.35×10^{-8} mol/cm^2, the short-circuit and power conversion efficiency of device D were higher than those of the STD device (made using conventional film). These results suggested that light scattering had a stronger influence than the dye amount on the performance of device D. The same conclusions could be derived from the IPCE spectra (Fig 9): the quantum efficiencies of the STD, A and D devices were all maximized to ~ 550 nm after the application of the D719 dye. The peak quantum efficiency of device D was almost equal to that of the STD device, but it was higher within the longer wavelength region (between ~ 560–700 nm). The higher efficiency in this spectral region could have been linked to a stronger scattering effect, induced by the formation of bigger TiO_2 aggregations. Since device A possessed the highest amount of dye and well scattering effect, it also presented the highest quantum efficiency over the whole spectral range, the highest power conversion efficiency (4.47 %), and a 23 % increase in J_{sc} compared to the STD device.

In addition, the quantum efficiency of device D in the shorter wavelength region of the IPCE spectrum was lower than that of other devices. Perhaps, this was due to the higher porosity and bigger pores of film D, derived from the larger size of its TiO_2 aggregations. When the incident light stroke on the film, the longer wavelengths were surely well scattered, but the shorter wavelengths were perhaps not properly scattered, due to the high structural porosity of the film itself. However, the photons deriving from the shorter wavelength regions could have been reflected forward due to the relatively high thickness of the film: there were enough chances to be reflected. Such mechanism would explain why device D presented a lower quantum efficiency, but not a lower reflectance than other films in the shorter wavelength region.

Table 1 Peformance of DSSCs

Sample	Adsorbed Dye ($\times 10^{-8}$ mol/cm^2)	Scattering effect (525nm)	J_{sc} (mA/cm^2)	V_{oc} (V)	FF	η (%
STD	6.35	weak	9.50	0.58	0.69	3.79
Device A	6.46		11.65	0.59	0.65	4.47
Device B	5.92		9.41	0.59	0.65	3.64
Device C	5.56		9.49	0.57	0.68	3.71
Device D	5.81	strong	10.63	0.58	0.66	4.08

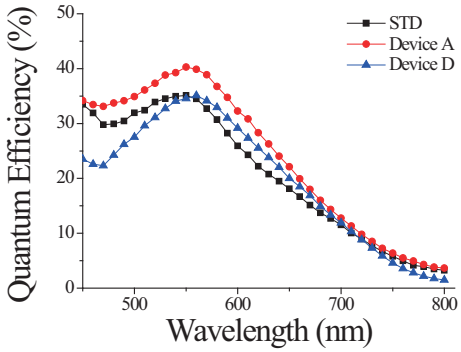

Fig 9 incident photo to current conversion efficiency spectra of DSSCs.

Conclusions

In this study, we prepared and characterized a series of hierarchically structured TiO_2 photoanodes. The analyses indicated that the J_{sc} tended to increase with the scattering effect in films characterized by increasingly larger TiO_2 aggregations. In our study, higher J_{sc} values corresponded to a more efficient light scattering in the photoanodes, although the amount of adsorbed dye decreased. The optimized device A, created using a PVA (MW = 31,000)-treated film, presented the highest dye loading, well light harvesting (resulting in a 23 % increase of the J_{sc}), and power conversion efficiency (4.47 %).

References

[1] B. O'Regan, M. Grätzel, A low-cost, high-efficiency solar cell based on dye-seneitized colloidal TiO_2 films, Nature 353 (1991) 737-740.

[2] M. Grätzel, Dye-sensitized solar cells, J. Photochem. Photobiol., C 4 (2003) 145-153.

[3] K.–M. Lee, V. Suryanarayanan, K.–C. Ho, A study on the electron transport properties of TiO_2 electrodes in dye-sensitized solar cells, Sol. Energy Mater. Sol. Cells 91

ISBN: 978-1-7281-2501-5

(2007) 1416-1420.
[4] L. Hu, S. Dai, J. Weng, S. Xiao, Y. Sui, Y. Huang, S. Chen, F. Kong, X. Pan, L. Liang, K. Wang, Microstructure design of nanoporous TiO_2 photoelectrodes for dye-sensitized solar cell modules, J. Phys. Chem. B 111 (2007) 358-362.
[5] O. K. Varghese, M. Paulose, C. A. Grimes, Long vertically aligned titania nanotubes on transparent conducting oxide for highly efficient solar cells, Nature Nanotech. 4 (2009) 592-597.
[6] J. Qian, P. Liu, Y. Xiao, Y. Jiang, U. Cao, X. Ai, H. Yang, TiO_2-coated multilayered SnO_2 Hollow microspheres for dye-sensitized solar cells, Adv. Mater. 21 (2009) 3663-3667
[7] H. Yu, S. Zhang, H. Zhao, B. Xue, P. Liu, G. Will, High-performance TiO_2 Photoanode with an efficient electron transport network for dye-sensitized solar cells, J. Phys. Chem. C 113 (2009) 16277-16282.
[8] M. Grätzel, Recent advances in sensitized mesoscopic solar cells, Acc. Chem. Res. 42 (2009) 1788-1798.
[9] J. Yu, J. Fan, L. Zhao, Dye-sensitized solar cells based on hollow anatase TiO_2 spheres prepared by self-transformation method, Electrochim. Acta 55 (2010) 597-602.
[10] U. O. Krašovec, M. Berginc, M. Hočevar, M. Topič, Unique TiO_2 paste for high efficiency dye-sensitized solar cells, Sol. Energy Mater. Sol. Cells 93 (2009) 379-381.
[11] Z. Wang, H. Kawauchi, T. Kashima, H. Arakawa, Significant influence of TiO_2 photoelectrode morphology on the energy conversion efficiency of N719 dye-sensitized solar cell, Coord. Chem Rev. 248 (2004) 1381-1389.
[12] Y. Zhao, J. Zhai, S. Tan, L. Wang, L. Jiang, D. Zhu, TiO_2 micro/nano-composite structured electrodes for quasi-solid-state dye-sensitized solar cells, Nanotechnology 17 (2006) 2090-2097.
[13] Y. J. Kim, M. H. Lee, H. J. Kim, G. Lim, Y. S. Choi, N. Park, K. Kim, W. I. Lee, Formation of highly efficient dye-sensitized solar cells by hierarchical pore generation with nanoporous TiO_2 spheres, Adv. Mater. 21 (2009) 3668-3673.
[14] J. Ferber, J. Luther, Computer simulations of light scattering and absorption in dye-sensitized solar cells, Sol. Energy Mater. Sol. Cells 54 (1998) 265-275.
[15] S. Hore, C. Vetter, R. Kern, H. Smit, A. Hinsch, Influence of scattering layers on efficiency of dye-sensitized solar cells, Sol. Energy Mater. Sol. Cells 90 (2006) 1176-1188.
[16] S. Nunomura, A. Minowa, H. Sai, M. Knodo, Mie scattering enhanced near-infrared light response of thin-film silicon solar cells, Appl. Phys. Lett. 97 (2010) 063507.
[17] Z. Tian, H. Tian, X. Wang, S. Yuan, J. Zhang, X. Zhang, T. Yu, Z. Zou, Multilayer structure with gradual increasing porosity for dye-sensitized solar cells, Appl. Phys. Lett. 94 (2009) 031905.

ISBN: 978-1-7281-2501-5